THE OPERATION OF A ROTATING, WICKLESS HEAT PIPE

by

Leonard John Ballback

United States
Naval Postgraduate School

THESIS

THE OPERATION O. A ROTATING, WICKLESS

HEAT PIPE

by

Leonard John Ballback

December 1969

The Operation of a Rotating, Wickless Heat Pipe

by

Leonard John Ballback
Lieutenant, United States Navy
B. S., United States Naval Academy, 1964

Submitted in partial fulfillment of the
requirements for the degrees of

MECHANICAL ENGINEER

and

MASTER OF SCIENCE IN MECHANICAL ENGINEERING

from the

NAVAL POSTGRADUATE SCHOOL
December 1969

ABSTRACT

A Nusselt type analysis was performed during laminar film condensation on the inside of a rotating truncated cone. This analysis was employed to determine the condensing limit of a wickless heat pipe, rotating about its longitudinal axis.

Performance characteristics including the effects of geometry, rotational speed, and the characteristics of fluid are given. A comparison is made between the condensing, boiling, sonic, and entrainment limits for a given heat pipe geometry.

TABLE OF CONTENTS

TABLE OF SYMBOLS

A	cross sectional area for flow, ft^2
A_b	heat transfer area in the boiler, ft^2
A_c	heat transfer area in the condenser, ft^2
C, C_1, C_2, C_3	arbitrary constants
C_p	specific heat at constant pressure, BTU/lbm deg F
d	depth of the boiler section (boiler exit radius minus boiler wall radius) ft
g	acceleration of gravity, ft/hr^2
F, G	dimensionless velocity parameters
h	local heat transfer coefficient, BTU/hr ft^2 deg F
h_m	mean heat transfer coefficient, BTU/hr ft^2 deg F
h_o	coolant heat transfer coefficient, BTU/hr ft^2 deg F
h_{fg}	latent heat of vaporization, BTU/lbm
k_f	thermal conductivity of the condensate film, BTU/hr ft deg F
k_w	thermal conductivity of the wall, BTU/hr ft deg F
L_c	length along the wall of the condenser, ft
$\dot{m}_f$	mass flow rate of fluid, lbm/hr
$\dot{m}_v$	mass flow rate of vapor, lbm/hr
N	"the figure of merit" of a working fluid, $BTU/hr^{\frac{1}{2}}$ ft deg $F^{3/4}$
P	pressure, lbf/ft^2
P_S	saturation pressure, lbf/in^2 or lbf/ft^2
P_v	pressure of the vapor, lbf/ft^2
q_t	total heat transfer rate, BTU/hr
r	radius, ft

R_o	minimum wall radius in the condenser section, ft
t	container wall thickness, ft
T_f	coolant temperature, deg F
T_s	saturation temperature, deg F
T_w	inside wall temperature, deg F
T_{wo}	outside wall temperature, deg F
u	average velocity of the fluid, ft/hr
u_f	velocity of the fluid, ft/hr
u_v	velocity of the vapor, ft/hr
U	characteristic velocity of the problem parallel to the surface, ft/hr
v	velocity normal to the surface, ft/hr
V	characteristic velocity of the problem normal to the surface, ft/hr
X	co-ordinate measuring distance along surface, ft
Y	co-ordinate measuring distance normal to surface, ft

GREEK

γ	characteristic height of the problem, ft
δ	film thickness, ft
η	dimensionless independent variable
μ_f	viscosity of fluid, lbm/ft hr
ρ_f	density of fluid, lbm/ft^3
ρ_v	density of vapor, lbm/ft^3
σ	surface tension, lbf/ft
τ	shear stress, lbf/ft^2
ϕ	half cone angle, rad
ω	angular velocity, 1/hr
ν	kinematic viscosity, ft^2/hr

SUBSCRIPTS

b	refers to boiler
c	refers to condenser
f	refers to fluid condition
m	refers to mean value
o	refers to a minimum value
s	refers to a saturated condition
t	refers to total
v	refers to the vapor condition
w	refers to the condenser wall
wo	refers to outside of the condenser wall

ACKNOWLEDGEMENTS

The author would like to express his appreciation to Dr. P. J. Marto of the Naval Postgraduate School for suggesting the project and his constructive criticisms of this work. The author would also like to thank Dr. M. D. Kelleher and Dr. R. H. Nunn for their perusal of the manuscript as the departmental readers.

I. INTRODUCTION

A. BACKGROUND

In recent years considerable interest has been generated in the study of capillary-pumped heat pipes as a means of transferring large quantities of heat. At present, for most pipes using ordinary fluids, the limit on the heat transfer appears to be the rate that the condensate can be returned to the evaporator [1]. The capillary-pumped heat pipes are primarily limited by the small pressure differentials obtainable across the meniscus of the liquid in the wicking, which gives rise to the pumping force. This differential pressure must overcome the losses of the liquid flowing in the wick, the losses in the vapor flow, and, depending on the orientation, the gravitational forces. A second limit, the onset of nucleate boiling in the evaporator portion of the wicking structure, may disrupt the capillary flow [2], [3]. Nucleate boiling will cause the formation of bubbles in the liquid condensate. These bubbles may then become trapped in the wicking structure, thus impeding the return flow and limiting the operation of the pipe [2], [3].

The limitations of the capillary-pumped heat pipes can be overcome through the use of centrifugal acceleration [4]. A pipe, rotating about its longitudinal axis, will generate its own gravitational field, independent of orientation, and thereby force the condensate to return to the boiler.

A rotating heat pipe is a closed hollow shaft which contains a working fluid. Rotation about its longitudinal axis generates a rotational force field. The rotational acceleration, together with a slight internal wall taper, pumps the working fluid from the condenser to the boiler

section. There is no porous wick structure as in a capillary heat pipe. The operation of a rotating heat pipe is shown schematically in Fig. 1.

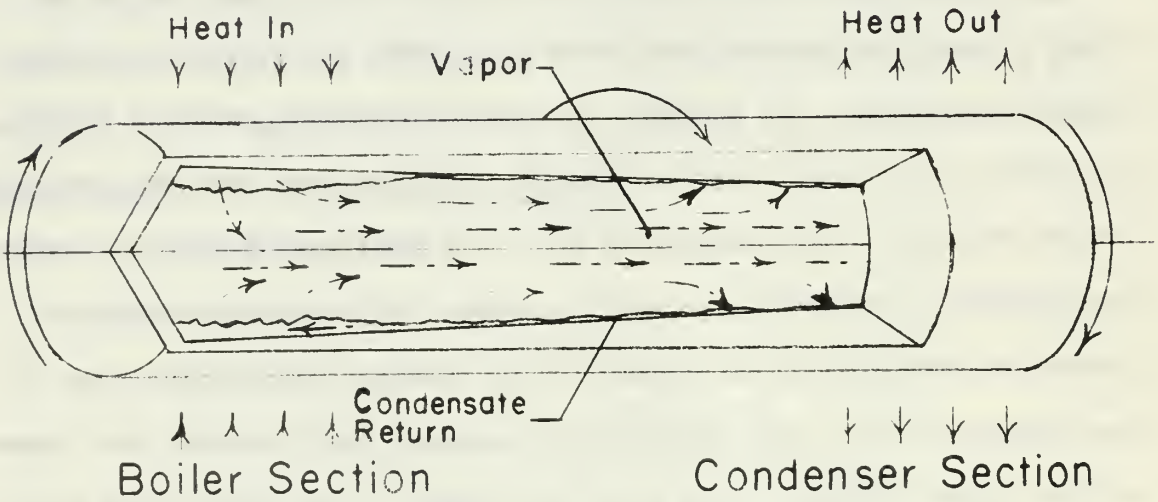

Figure 1. Cutaway View of Typical Rotating Heat Pipe

As the pipe is rotated, an annulus of working fluid is formed at the largest internal radius of the shaft. Heat is applied to this portion of the pipe. As heat is applied, the fluid evaporates or boils, forming a vapor. This vapor is then at a higher pressure than that at the narrower end of the pipe (condenser). This pressure differential forces the vapor from the boiler to the condenser section. Heat is removed at the condenser section, causing the vapor present at that section to condense on the walls of the shaft. The centrifugal force generated by the rotational motion of the pipe insures that the condensate will return to the boiler section. Thus the rotating heat

pipe has a closed, two-phase heat transfer cycle, and the flow of the condensate is not retarded by the porous wick structure.

The rotating heat pipe may be applied wherever there is a rotating part and a need to transfer heat. A few applications of the rotating heat pipe are the cooling of: a high speed drill, the rollers for a conveyer table of hot metals, the rotors of electric motors, and turbine blading.

B. THESIS OBJECTIVES

The objectives of this study were: a) to understand the operational principles, b) to develop an analytical model and, c) to predict the performance characteristics of a rotating heat pipe.

II. LIMITS OF OPERATION

As in the capillary heat pipes, the heat transfer limits of the rotating heat pipe are controlled primarily by fluid dynamic considerations.[5]. The effect of the following limits will be discussed: a) the boiling limit, b) the entrainment limit, c) the sonic limit, and d) the condensing limit.

A. BOILING LIMIT

When a surface is heated in a stagnant pool of saturated liquid, three basic regimes of heat transfer are observed to occur. In the low range of temperature differentials, $(T_w - T_s)$, the heat flux is low and the principle mechanism of heat transfer is free convection. As the temperature differential is increased, nucleate boiling becomes dominant. In this region, bubbles of the vapor are formed on the heating surface, grow in size, and eventually break off. After breaking away they rise to the surface and burst, releasing the vapor. The formation of the bubbles and their consequent rising agitates the liquid, causing convective currents to be set up. This agitation intensifies the heat transfer mechanism causing an upturn in the heat flux curve and increasing the heat transfer coefficient significantly. As the temperature differential is increased further, the bubbles become so numerous, that they begin to coalesce, and a film of vapor can then blanket the surface. The insulating effect of this vapor blanket makes the film boiling regime undesirable. A maximum heat flux exists for every boiler surface at which the transition occurs between nucleate boiling, and film boiling.

During the operation of the rotating heat pipe, the heat transfer coefficient, as mentioned above, will be increased due to nucleate boiling. A further increase in the coefficient will be experienced due to the rotational acceleration of the boiler [6], [7], [8]. The boiling limit in the rotating heat pipe will be reached upon the departure from nucleate boiling. This will occur as a sudden drop in the heat transfer coefficient which occurs when the maximum heat flux mentioned above has been reached. If the power input is held constant during this time, the surface temperature of the container will rapidly rise, usually causing the surface to melt. In the literature this phenomenon has been termed departure from nucleate boiling, boiling crisis, or burnout [9]. The boiling limit of the rotating heat pipe may be derived directly from the work done on conventional non-rotating boilers.

Kutateladze has postulated that the transition from nucleate boiling to film boiling is purely a hydrodynamic phenomenon [10]. Based on this assumption he has obtained the correlation formula for predicting the burnout heat flux.

$$\frac{q_t}{A_b} = K \sqrt{\rho_v}\, h_{fg} \left\{ \sigma\, g \left[\rho_f - \rho_v \right] \right\}^{1/4} \qquad (1)$$

where

q_t = total heat transfer, BTU/hr

A_b = heat transfer area in the boiler, ft^2

ρ_v = density of the vapor, lbm/ft^3

h_{fg} = latent heat of vaporization, BTU/lbm

σ = surface tension, lbf/ft

g = acceleration of gravity, ft/hr^2

ρ_f = density of the fluid, lbm/ft^3

Kutateladze's experimental data indicates the average value of K is .14, obtaining from a range of .13 to .19 for various surface conditions of horizontal wires and discs [11]. A counterflow configurattion of inviscid vapor and liquid jets in the high nucleate boiling regime was proposed by Zuber, Tribus, and Westwater to predict the burnout point [12]. Their results for the burnout heat flux on a flat plate heater shows that K is equal to $\pi/24$ (or .13). Experimenters have substantiated Kutateladze's formula and have shown that the burnout heat flux increases for rotation approximately as the rotational acceleration to the one fourth power [13], [14]. Thus the boiling limit of the rotating heat pipe may be adequately described by the correlation formulas of Kutateladze and Zuber [9], [15]. The heat flux equation (1) may be recast as a heat rate by multiplying through by the surface area of the rotating heat pipes boiler. This gives equation (2)

$$q_t = K \sqrt{\rho_v}\, h_{fg} A_b \left\{ \sigma g \left[\rho_f - \rho_v \right] \right\}^{1/4} \qquad (2)$$

where

$$K = .13 - .19$$

B. ENTRAINMENT LIMIT

During the operation of the rotating heat pipe, a counter current flow of the liquid condensate along the walls and vapor in the central core of the pipe is set up. A shearing off of the condensate by the vapor,holding up the condensate and thereby causing the vapor formation in the boiler to exceed the condensate return, will be defined as the entrainment limit. High heat fluxes during steady state operation and certain critical heat fluxes during start up conditions may possibly generate counter current (vapor-condensate) flow rates capable of

triggering entrainment of the condensate. In counter current flow, a condition closely related to the entrainment problem has been defined in the literature as flooding [16]. When this condition is reached, it is impossible to increase the flow rate of the liquid component without making a corresponding decrease in the flow rate of the vapor component and vice versa. Hewitt, Lacey, and Nicholls have shown that the flow contact length is a strong parameter for the flooding transition at high liquid flow rates. They also have shown experimentally that as the absolute pressure is increased, the flow rates attainable before the flooding transition are higher [17]. In order to understand the statements and results of Hewitt, Lacey, and Nicholls, this discussion of droplet entrainment from a liquid film for co-current annular flow by C. B. Wallis is presented:

> "For any given liquid flow rate the gas-liquid interface is characterized by the following physical appearance. At zero gas velocity the liquid has a smooth, mirror-like appearance as it moves along the duct. At a low gas velocity the surface starts to break up into a ripple pattern. As the gas velocity is further increased, the ripples start to bunch up and a wave is produced which appears to move at a velocity several times that of the entrained film. This wave, referred to as a roll wave, moves down the duct on top of the entrained film. At still higher gas velocities these roll waves grow smaller (yet more frequent) and droplet entrainment becomes evident. These waves are a precondition for the onset of entrainment and the source of the droplets. The wave tops are sheared off by the gas flowing over them. The roll waves appear to 'roll' in the direction of the gas flow." [18]

The rotational acceleration in the rotating heat pipe will be a significant parameter in suppressing the formation of a rolling wave as described by Wallis [18]. It should act in the same manner as the increased absolute pressure delayed the onset of flooding in the experiments of Hewitt, Lacey, and Nicholls [17]. In addition, since the rotating heat pipe is a sealed, self contained unit, the internal pressure may be

regulated to such a value as to ensure no liquid entrainment will occur.

At the present time there is no satisfactory theory available to predict the onset of entrainment, but the experimental data of Hewitt, et al, can be used to predict the entrainment limit [17].

C. SONIC LIMIT

As the heat flux in the rotating heat pipe is increased, it is possible that the flow rate of the vapor down the container may be limited by the attainment of a choked flow condition for the vapor. This choking of the vapor flow will definitely limit the amount of energy the vapor can transport down the pipe, thus limiting the operation of the pipe. The heat transfer mechanism employed in the rotating heat pipe depends on the latent energy of the working fluid. The heat transfer rate in the pipe may then be expressed as

$$q_t = \dot{m}_v h_{fg} \tag{3}$$

where

$\dot{m}_v$ = mass flow rate of the vapor (lbm/hr)

From continuity, the mass flow rate of the vapor may be expressed by

$$\dot{m}_v = \rho_v u_v A \tag{4}$$

where

u_v = velocity of the vapor (ft/sec), and

A = cross sectional area for flow (ft^2)

Combining equations (3) and (4) yields

$$q_t = \rho_v u_v A h_{fg} \tag{5}$$

If the cross sectional area of the pipe is known where the choked condition occurs,[1] the sonic limitation on the heat rate may then be computed using equation (5) with the vapor velocity taken as the sonic velocity.

D. CONDENSING LIMIT

The condenser may limit the rate of return of the condensate to the boiler by two mechanism; a) the rate that energy may be extracted from the system, and b) the maximum flow rate of the condensate. At the present no solution exists in the literature for condensation on a truncated cone. The solution for condensation on a rotating cone has been carried out by Sparrow and Hartnett [19]. Their solution employs a boundary layer similarity approach. As is stated by Sparrow and Hartnett, the solution applies only to cones that are not too slender and in a region sufficiently removed from the apex of the cone. As can be seen in Fig. 1, the rotating heat pipe will generally employ a slender, truncated cone for a condenser section. If Sparrow and Hartnett's solution for condensation on a cone were employed, then the boundary condition of the rotating heat pipe would not be fulfilled, namely that the velocity of the condensate is zero at the narrowest section of the condenser. Hence, a truncated cone solution is necessary. However, since a similarity solution for the truncated cone would not apply in the region near the narrow end of the condenser, due to the boundary layer assumptions, the following Nusselt-type analysis was made.

---

[1] As slender pipes are anticipated (small cone angles) then as a good first approximation, it can be assumed that choked flow occurs at the exit area of the boiler.

III. THEORETICAL ANALYSIS OF FILM CONDENSATION ON THE INSIDE OF A ROTATING-TRUNCATED CONE

In attacking the problem of condensation on the inside of a truncated cone the following assumptions are made.

A. ASSUMPTIONS

a) Film condensation, not dropwise condensation, occurs in the condenser section. Thus the condensing liquid wets the container surface and condensation occurs at a sufficient rate to allow a continuous film over the surface. The assumption of filmwise condensation is felt to be the conservative choice as dropwise condensation has been shown to give higher heat transfer rates [20].

b) The film of condensate undergoes laminar flow. Cannon and Kays, using a pipe rotating about its longitudinal axis with annular flow, have reported,

> "Tube rotation apparently has the effect of stabilizing a laminar flow so that a higher through-flow Reynolds number is obtained before transition occurs." [21].

c) The fluid properties are constant. Heat pipes are normally operated as nearly isothermal devices. This condition should be easily achieved in the rotating system and thus the fluid properties will very nearly be a constant.

d) The subcooling of the condensate may be neglected. A small correction factor is normally applied to the latent heat of vaporization term in order to take into account the effect of subcooling. The necessity for this correction is determined by the comparison of the term $C_p \Delta T$ (C_p is the specific heat at constant pressure, BTU/lbm deg F, and ΔT is the difference between the wall temperature and the saturation

temperature, deg F) with the latent heat of vaporization. Normally $C_p \Delta T$ is much less than h_{fg} and thus may be neglected.

e) The momentum changes through the condensate are small and thus there is essentially a static balance of forces. Sparrow and Gregg have shown that the momentum effects are negligible for ordinary fluids in laminar film condensation on a flat plate [22]. Assumption i), a thin film, also indicates that momentum changes may be neglected.

f) The vapor exerts no drag on the motion of the condensate; there is no interfacial shear. Experiments have shown that for Prandtl numbers of ten and higher the effect on heat transfer of interfacial shear is negligible. For Prandtl numbers near one the effect is only slight (within five percent) [23].

g) There is a linear distribution of temperature through the condensate film. Rohsenow has shown that for Prandtl numbers above one, the non-linear distribution of temperature through a thin film, due to energy convection, is hardly distinguishable [24]. Thus energy convection is neglected and heat transfer occurs by conduction only.

h) The centrifugal force is much greater than the force of gravity and thus gravity may be neglected.

i) The thickness of the film is much less than the radius of curvature of the condenser wall.

j) The vapor space is essentially at one pressure, P_v. There is no radial distribution of pressure in the vapor space and the axial distribution of pressure is nearly a constant [25], [26].

k) The density of the fluid is much greater than the density of the vapor.

l) The rotating heat pipe is operating at a steady state condition.

m) Velocity gradients in the circumferential direction relative to the pipe wall are negligible.

By using the above assumptions and the coordinate system shown in Fig. 2, an analysis similar to Nusselt's original film condensation theory may be used [27].

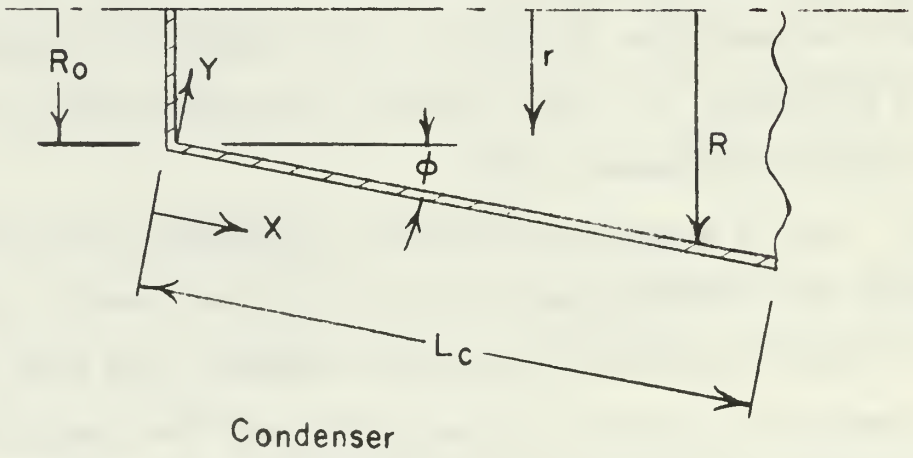

Figure 2. Coordinate System and Geometry for Condensing Limit

A force balance may be taken on an infinitesimal fluid element in the X-direction as shown in Fig. 3. This leads to an expression for the momentum equation within the condensate.

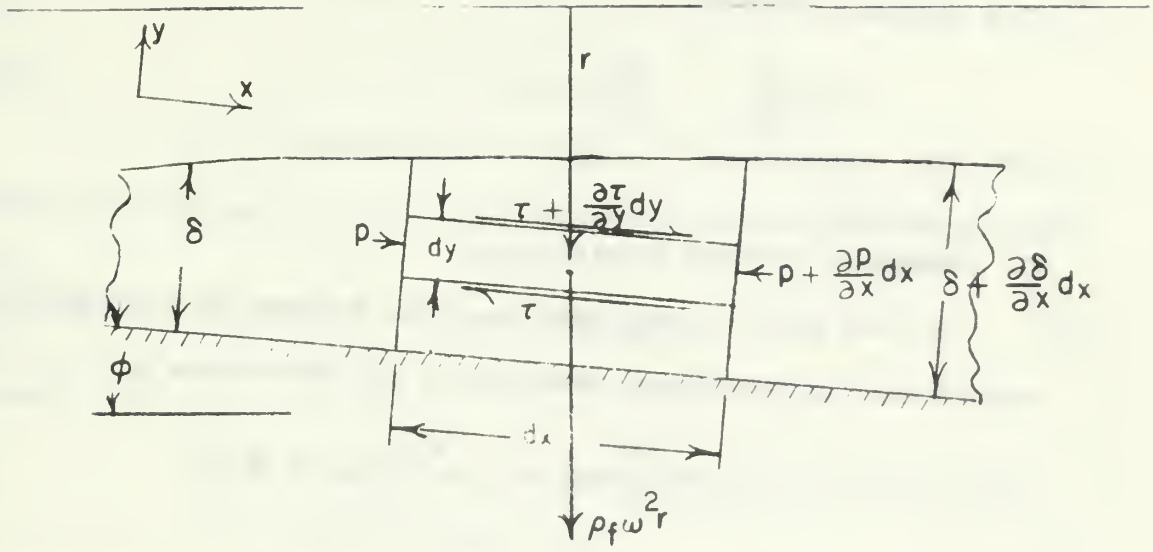

Figure 3 Force Balance in X-Direction on an Infinitesimal Fluid Element

B. MOMENTUM EQUATION (X-direction)

$$\sum F_x = 2\pi r P dy - 2\pi r \left\{P + \frac{\partial P}{\partial x} dx\right\} dy - \tau 2\pi r dx + \left\{\tau + \frac{\partial \tau}{\partial y} dy\right\} 2\pi r dx + \rho_f \omega^2 2\pi r^2 dx dy \sin\phi \quad (6)$$

where

P = pressure, (lbf/ft^2)

r = radius, (ft)

X = co-ordinate measuring distance along the surface, (ft)

Y = co-ordinate measuring distance normal to surface, (ft)

τ = shear stress, (lbf/ft^2)

ϕ = half cone angle (rad)

ρ_f = density of fluid, (lbm/ft^2), and

ω = angular velocity, (1/hr)

This equation reduces to

$$0 = \frac{\partial \tau}{\partial y} - \frac{\partial P}{\partial x} + \rho_f \omega^2 r \sin\phi \tag{7}$$

C. MOMENTUM EQUATION (Y-direction)

In like manner, using Fig. 4, a force balance in the Y-direction, neglecting the centrifugal head due to the vapor since $\rho_f >> \rho_v$, gives:

$$\sum F_y = 2\pi r P\, dx - 2\pi r \left\{ P + \frac{\partial P}{\partial y} dy \right\} dx - \rho_f \omega^2 r 2\pi \cos\phi\, dx\, dy \tag{8}$$

This reduces to

$$0 = -\frac{\partial P}{\partial y} - \rho_f \omega^2 r \cos\phi \tag{9}$$

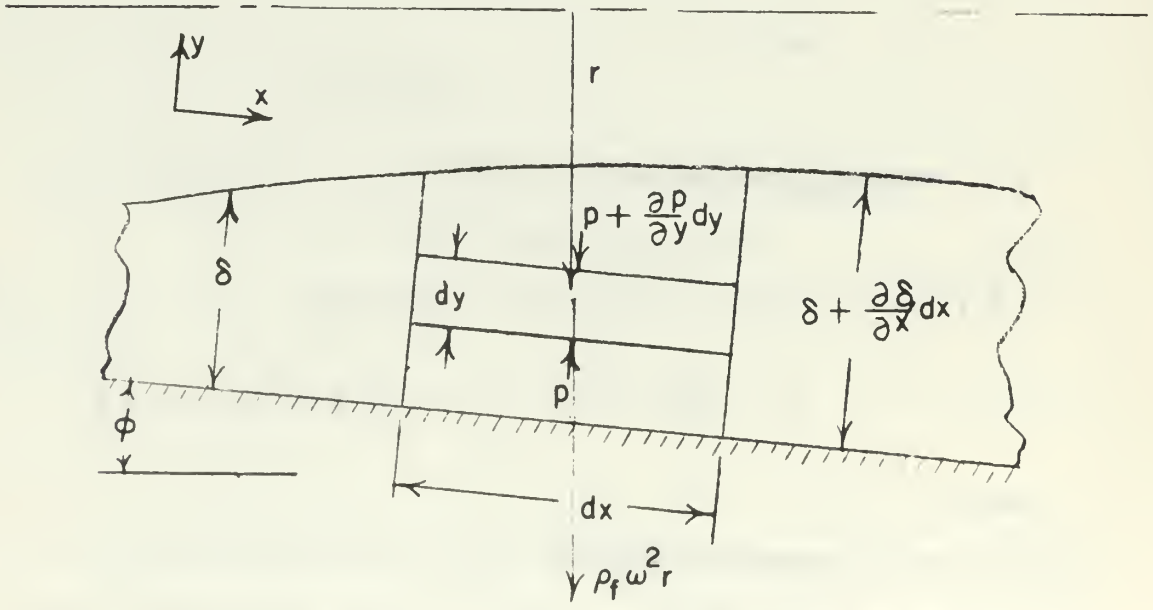

Figure 4. Force Balance in Y-Direction on an Infinitesimal Fluid Element

Making use of Fig. 2, the radius at any point in the fluid condensate may be expressed as

$$r(x,y) = R_o + X \sin\phi - Y \cos\phi \tag{10}$$

where

R_o = minimum wall radius in the condenser section (ft)

Substituting equation (10) into (9) for r(x,y) and integrating gives

$$\int_P^{P_v} \frac{\partial P}{\partial y}\, dy = -\rho_f \omega^2 \cos\phi \int_Y^{\delta} (R + X \sin\phi - Y \cos\phi)\, dy \tag{11}$$

where

P_v = pressure of the vapor (lbf/ft^2)

δ = film thickness (ft)

This yields

$$P = P_v + \rho_f \omega^2 \cos\phi \left\{ \left[R_o + X \sin\phi \right] \left[\delta - Y \right] - \frac{1}{2} \cos\phi \left[\delta^2 - Y^2 \right] \right\} \tag{12}$$

Now differentiating equation (12) with respect to X gives

$$\frac{\partial P}{\partial x} = \frac{dP_v}{dx} + \rho_f \omega^2 \cos\phi \left\{ R_o \frac{d\delta}{dx} + \delta \sin\phi + X \sin\phi \frac{d\delta}{dx} - Y \sin\phi - \delta \cos\phi \frac{d\delta}{dx} \right\} \tag{13}$$

If the result of equation (13), $\frac{\partial P}{\partial x}$, is substituted into equation (7) it becomes

$$0 = -\frac{dP_v}{dx} - \rho_f \omega^2 \cos\phi \left\{ R_o \frac{d\delta}{dx} + \delta \sin\phi + X \sin\phi \frac{d\delta}{dx} - Y \sin\phi - \delta \cos\phi \frac{d\delta}{dx} \right\} \tag{14}$$

$$+ \rho_f \omega^2 \sin\phi \left\{ R_o + X \sin\phi - Y \cos\phi \right\} + \frac{\partial \tau}{\partial y}$$

Integrating equation (14) over the limits from Y to δ and τ to 0, then rearranging yields

$$\mu_f \frac{\partial u_f}{\partial \quad} = -\frac{dP_v}{dx}\left\{\delta - Y\right\} - \quad \text{(15)}$$

$$-\delta\cos\phi \quad \left\{\delta - Y\right\} + \rho_f \omega^2 \sin\phi \quad \left\{ - Y\right\}$$

where in equation (15) for laminar flow

$$\tau = \mu_f \frac{\partial \quad}{\partial \quad}$$

and

u_f = velocity of the fluid, (ft/hr)

μ_f = viscosity of the fluid, (lbm/ft hr)

Equation (15) may now be solved for the velocity profile, u_f, by integration over the limits 0 to Y and 0 to u_f.

$$u_f = -\frac{1}{\mu_f}\frac{dP_v}{dx}\left\{\delta Y - \frac{Y^2}{2}\right\} - \frac{\rho_f \omega^2 \cos\phi}{\mu_f}\left\{P_0 \frac{d\delta}{dx} + \delta\sin\phi + X\sin\phi\frac{d\delta}{dx}\right. \quad \text{(16)}$$

$$\left. -\delta\cos\phi \quad \right\}\left\{\delta Y - \frac{Y^2}{2}\right\} + \frac{\rho_f \omega^2 \sin\phi}{\mu_f}\left\{P_0 + X\sin\phi\right\}\left\{\delta Y - \frac{Y^2}{2}\right\}$$

Applying assumption j), (vapor space at one pressure, P_v), allows equation (16) to be rewritten as

$$u_f = \frac{\rho_f \omega^2}{\mu_f}\left\{\delta Y - \frac{Y^2}{2}\right\}\left\{P_0 \quad \sin\phi - \cos\phi \frac{d\delta}{dx}\right] + X\sin\phi\left[\sin\phi - \cos\phi\frac{d\delta}{dx}\right] \quad \text{(17)}$$

$$\left. - \delta\cos\phi\left[\sin\phi - \cos\phi\frac{d\delta}{dx}\right]\right\}$$

Note that in equation (17) $u_f = u_f(x,y)$ since $\delta = \quad (x)$.

D. CONTINUITY EQUATION

The continuity equation of fluid dynamics requires that

$$\dot{m}_f = \rho_f \bar{u} A$$

where

$\dot{m}_f$ = mass flow rate of fluid, (lbm/hr)

$\bar{u}$ = average velocity of fluid, (ft/sec)

This can be written as

$$\dot{m}_f = \int_0^{\delta} \rho_f u_f 2\pi r \, dy \tag{18}$$

Substituting equation (17) into (18) and carrying out the integration

$$\dot{m}_f = \frac{2\pi\rho_f\omega^2}{\mu_f} \left\{ \left[R_0 + X\sin\phi - \delta\cos\phi \right] \frac{d}{dx}\left[R_0 + X\sin\phi - \delta\cos\phi \right] \right\} \tag{19}$$

$$\left\{ \frac{\delta^3}{3}\left[R_0 + X\sin\phi \right] - \frac{5}{24}\delta^4\cos\phi \right.$$

Utilizing assumption i) (thin film) allows equation (19) to become

$$\dot{m}_f = \frac{2\pi\rho_f^2\omega}{\mu_f} \frac{\delta^3}{3} \left\{ \left[R_0 + X\sin\phi \right] \sin\phi \right\} \tag{20}$$

Differentiating this result with respect to X gives

$$\frac{d\dot{m}_f}{dx} = \frac{2\pi\rho_f^2\omega}{\mu_f} \left\{ \left[R_0 + X\sin\phi \right] \sin\phi\,\delta^2 \frac{d\delta}{dx} + \frac{2}{3}\sin^2\phi\,\delta^3 \left[R_0 + X\sin\phi \right] \right\} \tag{21}$$

E. ENERGY EQUATION

If the film surface temperature is T_s and the wall is at T_w, then the heat transfer by conduction to an element of surface area dA_c is

$$dq_f = \frac{k_f \cos\phi \left\{T_s - T_w\right\} dA_c}{\left\{R_o + X\sin\phi\right\} \ln\left\{\frac{R_o + X\sin\phi}{R_o + X\sin\phi - \delta\cos\phi}\right\}} \qquad (22)$$

where

$dA_c = 2\pi\left\{R_o + X\sin\phi\right\} dx$

A_c = heat transfer area in the condenser, (ft)

k_f = thermal conductivity of the condensate film, (BTU/hr ft deg F)

T_s = saturation temperature, (deg F)

T_w = inside wall temperature, (deg F)

Therefore

$$dq_f = \frac{2\pi k_f \cos\phi \left\{T_s - T_w\right\} dx}{\ln\left\{\frac{R_o + X\sin\phi}{R_o + X\sin\phi - \delta\cos\phi}\right\}} \qquad (23)$$

which can be written as

$$dq_f = \frac{2\pi k_f \cos\phi \left\{T_s - T_w\right\} dx}{\ln\left\{1 - \frac{\delta\cos\phi}{R_o + X\sin\phi}\right\}} \qquad (24)$$

The assumption of a thin film, assumption i), gives

$$\frac{\delta\cos\phi}{R_o + X\sin\phi} << 1$$

Therefore

$$\ln\left\{1 - \frac{\delta\cos\phi}{R_o + X\sin\phi}\right\} \approx -\frac{\delta\cos\phi}{R_o + X\sin\phi}$$

Equation (24) then becomes

$$dq_f = \frac{k_f}{\delta} 2\pi \left\{ R_0 + X \sin \phi \right\} \left\{ T_s - T_w \right\} dx \qquad (25)$$

The rate of condensation is

$$dq_f = h_{fg} d\dot{m}_v \qquad (26)$$

Since the pipe is operating at a steady state condition, continuity for the entire system requires that

$$|\dot{m}_v| = |\dot{m}_f|$$

and applying this result to equation (26) gives

$$dq_f = h_{fg} d\dot{m}_f \qquad (27)$$

Equating equations (27) and (25), the mass rate of condensation per unit length is

$$\frac{d\dot{m}_f}{dx} = \frac{k_f}{\delta h_{fg}} 2\pi \left\{ R_0 + X \sin \phi \right\} \left\{ T_s - T_w \right\} \qquad (28)$$

Equating equations (28) and (21), then rearranging gives

$$\frac{k_f \mu_f \left\{ T_s - T_w \right\}}{\rho_f^2 \omega^2 h_{fg} \sin \phi} = \delta^4 \left\{ \frac{\left[R_0 + X \sin \phi \right]}{\delta} \frac{d\delta}{dx} + \frac{2}{3} \sin \phi \right\} \qquad (29)$$

F. FILM THICKNESS

Now carrying out this integration (see Appendix A) for δ , the final results are

$$\delta = \left\{ \frac{3}{2} \frac{k_f \mu_f \left\{ T_s - T_w \right\}}{\rho_f^2 \omega^2 \sin^2 \phi \, h_{fg}} \left[1 - \left\{ \frac{R_0}{R_0 + X \sin \phi} \right\}^{8/3} \right] \right\}^{1/4} \qquad (30)$$

The local heat transfer coefficient, h, (BTU/hr ft^2 deg F), is given by

$$h = \frac{k_f}{\delta} = \left\{ \frac{2}{3} \frac{k_f^3 \rho_f^2 \omega^2 \sin^2\phi\, h_{fg}}{\mu_f (T_s - T_w)} \frac{1}{\left\{1 - \left[\frac{R_o}{R_o + x \sin\phi}\right]^{3/4}\right\}} \right\}^{1/4} \qquad (31)$$

G. MEAN HEAT TRANSFER COEFFICIENT

The mean heat transfer coefficient over the whole surface area of the truncated cone is given by

$$h_m = \frac{1}{\pi L_c \{2R_o + L_c \sin\phi\}} \int_0^{L_c} 2\pi h \left[R_o + x \sin\phi \right] dx \qquad (32)$$

where

L_c = length along the wall of the condenser, (ft)

Integrating equation (32) (see Appendix B) yields

$$h_m = \frac{1}{\{2R_o + L_c \sin\phi\}} \left\{ \frac{2}{3} \frac{k_f^3 \rho_f^2 h_{fg} \omega^2 \sin^2\phi\, L_c^4 [T_s - T_w]}{\mu_f} \right\}^{1/4} \qquad (33)$$

IV. DETERMINATION OF THE CONDENSING LIMIT

The analysis of film condensation on a truncated cone may be applied to the condenser section of the rotating heat pipe. This then will give an equation which will predict the condensing limit for the rotating heat pipe. The total heat rate in the condenser, q_t, is given by

$$q_t = h_m \pi L_c \{T_s - T_w\} \{2R_o + L_c \sin\phi\} \tag{34}$$

The value of h_m is now substituted into equation (34) and

$$q_t = \pi \left\{ \frac{2}{3} \frac{k_f^3 \rho_f^2 \omega^2 h_{fg} \left[T_s - T_w\right]^3}{\mu \sin^2\phi} \right\}^{1/4} \left\{ \left[R_o + L_c \sin\phi\right]^{8/3} - R_o^{8/3} \right\}^{3/4} \tag{35}$$

This then is the operating equation for predicting the limiting heat rate for the condenser. In the equation, however, the quantity T_w is not a readily controllable quantity. The inside wall temperature will actually adjust to a temperature corresponding to the heat rate (the saturation temperature) and the outside wall temperature. As the heat rate in the rotating heat pipe is increased, the internal pressure and saturation temperature will increase, accordingly requiring that the inside wall temperature adjust for this increase. Thus, the outside wall temperature of the condenser will be the controllable and measurable quantity. The inside wall temperature, T_w, then may be found as a function of the outside wall temperature, T_{wo}, and the heat rate by use of Fourier's conduction law through the consenser wall,

$$dq_t = \frac{k_w}{t} 2\pi \left\{R_o + X \sin\mu\right\} \left\{T_w - T_{wo}\right\} dx \tag{36}$$

where

k_w = thermal conductivity of the wall, (BTU/hr ft deg F)

t = condenser wall thickness, ft

Once again the cylindrical effects have been neglected due to the thin wall of thickness t. Integrating equation (36) from 0 to q_t and 0 to L_c yields

$$q_t = \frac{k_w}{t} 2\pi L_c \{T_w - T_{wo}\} \{R_o + \frac{L_c}{2} \sin\phi\} \qquad (37)$$

A. OPERATING EQUATIONS

The operating equation for the condensing limit is then an iterative solution between equation (35) and (37).

$$q_t = \pi \left\{ \frac{2}{3} \frac{k_f^3 \rho_f^2 \cdot h_{fg} \left[T_s - T_w\right]^3}{\mu_f \sin^2 \phi} \right\}^{1/4} \left\{ \left[R_o + L_c \sin\phi\right]^{8/3} - R_o^{8/3} \right\}^{3/4} \qquad (35)$$

$$q_t = \frac{k_w}{t} 2\pi L_c \{T_w - T_{wo}\} \{R_o + \frac{L_c}{2} \sin\phi\} \qquad (37)$$

At this point it should be noted that although operating equations for the condensing limit of the pipe itself have been derived, as an engineering consideration, the outside cooling mechanism for the pipe is extremely important. Indeed, it may become the limiting consideration. This then gives a third equation to be satisfied.[2]

$$q_t = h_o 2\pi L_c \{T_{wo} - T_\infty\} \{R_o + \frac{L_c}{2} \sin\phi\} \qquad (38)$$

---

[2]This is assuming that the film and wall thicknesses are very thin, and thus the areas are approximately equal.

where

h_o = coolant heat transfer coefficient (BTU/hr ft^2 deg F)

T_f = coolant temperature, (deg F)

V. PREDICTED PERFORMANCE CHARACTERISTICS

In the actual application of the rotating heat pipe, various methods of cooling the condenser section are anticipated. The assumption is made here, however, that the cooling mechanism employed is capable of setting the outside surface temperature of the condenser at a constant value, T_{wo}. Equation (38) is thus eliminated from the solution. Rearranging the remaining condensing limit equations gives

$$q_f = \pi \left\{\frac{2}{3}\right\}^{1/4} \left\{\frac{k_f^3 \rho^2 h_{fg}}{\mu_f}\right\}^{1/4} \left\{\omega^2 \left[T_s - T_w\right]\right\}^{1/4} \left\{\frac{\left[R_o + L_c \sin\phi\right]^{8/3} - R_o^{8/3}}{\sin^{2/3}\phi}\right\}^{3/4} \qquad (35)$$

$$q_f = 2\pi\, k_w \left\{T_w - T_{wo}\right\} \frac{L_c}{t} \left\{R_o + \frac{L_c}{2} \sin\phi\right\} \qquad (37)$$

These equations are a function of the physical properties of the working fluid, the thermal conductivity and the geometry of the pipe, and the operating conditions of rotational angular velocity and outside wall temperature T_{wo}.

A rotating heat pipe with the physical dimensions as shown in Fig. 5 was chosen in order to demonstrate the predicted performance of a given pipe. The boiler section was modeled as shown in Fig. 5 in order to insure that an adequate supply of working fluid would be available for an actual pipe. Also with this model the rotating heat pipe boiler is closely approximated by the rotating boiler tested at Lewis Research

Center [7]. The results of the Lewis tests can be used to design and check the operation of the rotating heat pipe boiler.

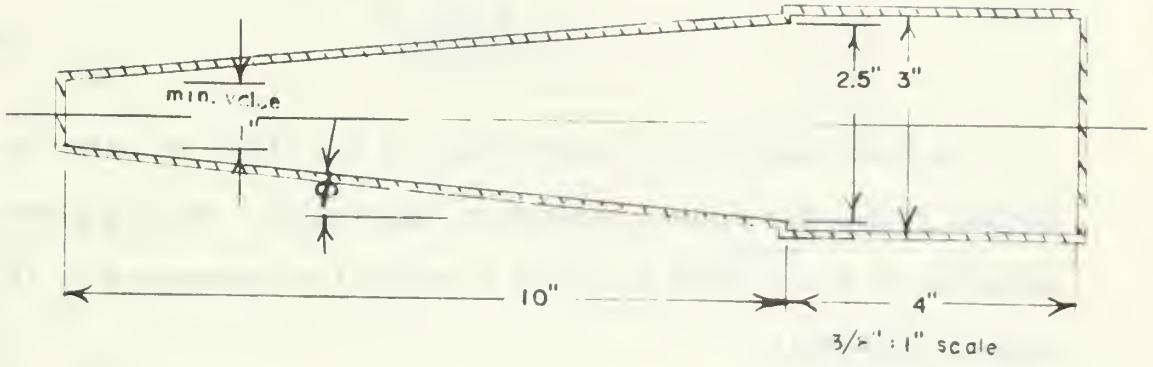

Figure 5. Simplified Model of a Rotating Heat Pipe

The outside wall temperature of the condenser, T_{wo} was chosen as 70 degrees Fahrenheit. For the saturation temperature of a particular fluid, the fluid properties were determined. An IBM Dual 360 digital computer was employed in iteratively solving the condensing limit equations (35) and (37). For a given angle, ϕ, and rotational speed, ω , the inside wall temperature, T_w, was varied until the heat rates of equations (35) and (37) agreed within 10 BTU per hour. It should be noted that the condenser length, 10 inches, and the radius of the boiler exit, 1.25 inches, were held constant while the angle ϕ was varied.

A. EFFECT OF FLUIDS

The choice of the working fluid in a rotating heat pipe is dependent upon several physical properties of the fluid as well as the operating conditions desired. Various working fluids may be compared by the use of a dimensional parameter, N, defined as "the figure of merit."

$$N = \left\{ \frac{k_f^3 \rho_f^2 h_{fg}}{\mu_f} \right\}^{1/2} \tag{39}$$

The heat rate will be proportional to the figure of merit of various fluids for a given saturation temperature. Table I gives the variation in N for three fluids at a saturation temperature of 122 degrees Fahrenheit.

TABLE I

Figure of Merit

Fluid	N
Water	20
Ethyl Alcohol	5
Freon 12	2.4

It should be noted that for ordinary fluids, water is the most desirable working fluid. This is primarily due to the combination of a relatively high thermal conductivity (which is cubed) coupled with a high latent heat of vaporization.

The vaporization curve of a given fluid will determine the operating temperature range of the fluid. The heat rate attainable will then be determined by the choice of fluid and the operating temperature of the pipe as shown in Fig. 6. It should be noted that in Fig. 6 the geometry

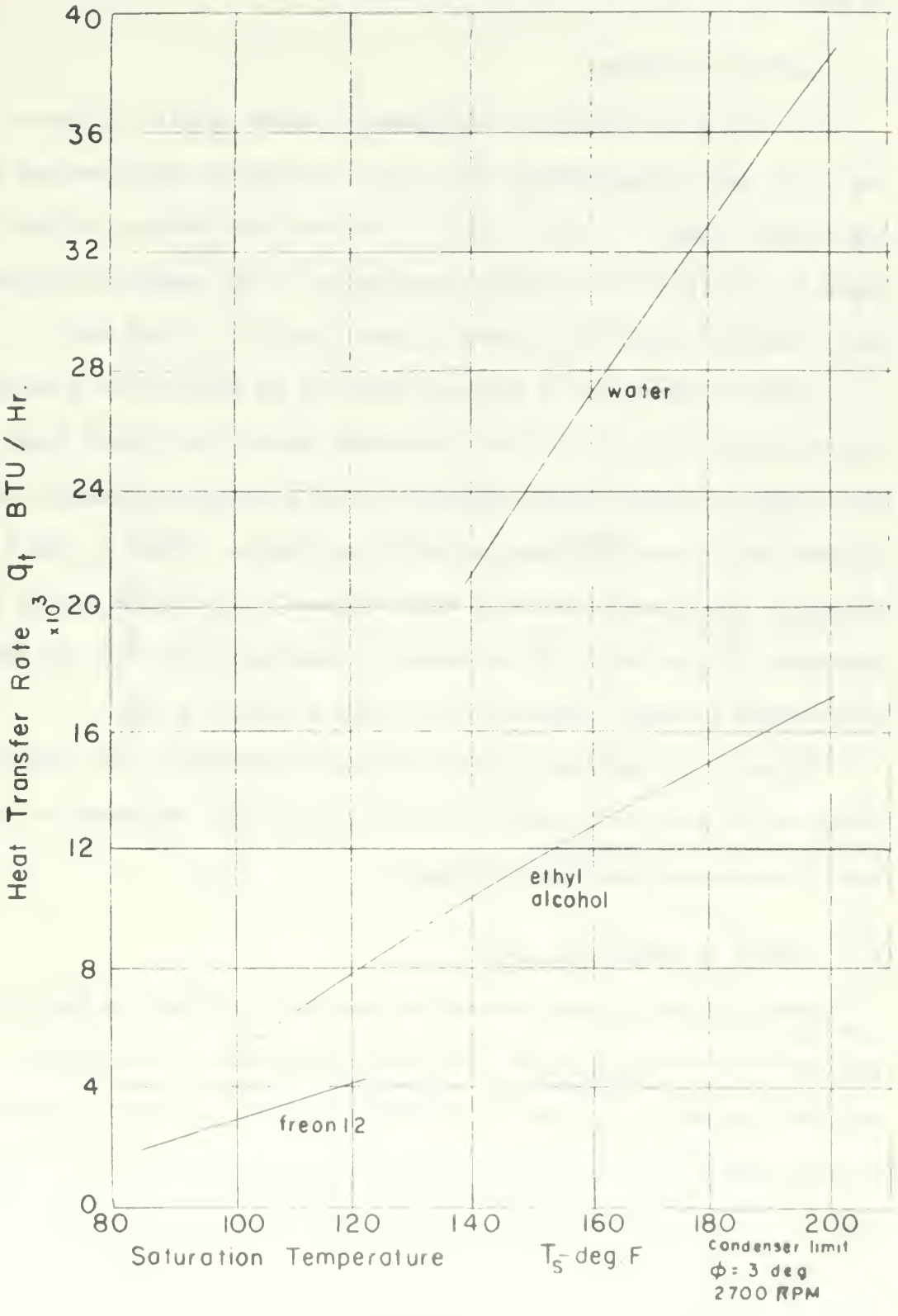

Figure 6 Heat Transfer Rate vs Saturation Temperature for Various Fluids

of the rotating heat pipe is as shown in Fig. 5 with a constant rotational speed of 2700 RPM, and the half cone angle, $\emptyset$, of 3 degrees.

B. EFFECT OF GEOMETRY

For the given geometric configuration shown in Fig. 5 the half cone angle, $\emptyset$, was allowed to vary for a given operating condition and working fluid. Figure 7 shows a plot of the heat rate versus the half cone angle for water at a saturation temperature of 212 degrees Fahrenheit. The rotational speed was allowed to vary from 300 to 3000 RPM.

Figure 7 shows that a maximum heat rate is achieved at a particular half cone angle for a given rotational speed (the dotted line). This peaking is due to the model used. The boiler exit diameter was held constant while the half cone angle, $\emptyset$, was varied. Since $L_c \cos \emptyset$, the condenser axial length was also held constant, the minimum radius of the condenser, R_o, varied. As $\emptyset$ increased R_o decreased and thus the heat rate versus the half cone angle curve has a maximum point.

Figure 7 illustrates that for the model chosen, as the rotational speed of the pipe is increased, the half cone angle necessary to maintain the maximum heat rate decreases.

C. EFFECT OF ROTATIONAL SPEED

The rotational speed versus the heat rate is shown in Fig. 8 for various half cone angles, $\emptyset$. This curve is presented for water at 212 degrees Fahrenheit in order to determine the most desirable operating speed range. One of the assumptions for the condensation on a truncated cone was that the centrifugal force is much greater than the gravity force (assumption h). For the model shown in Fig. 5, this condition is estimated to occur at approximately 700 RPM.

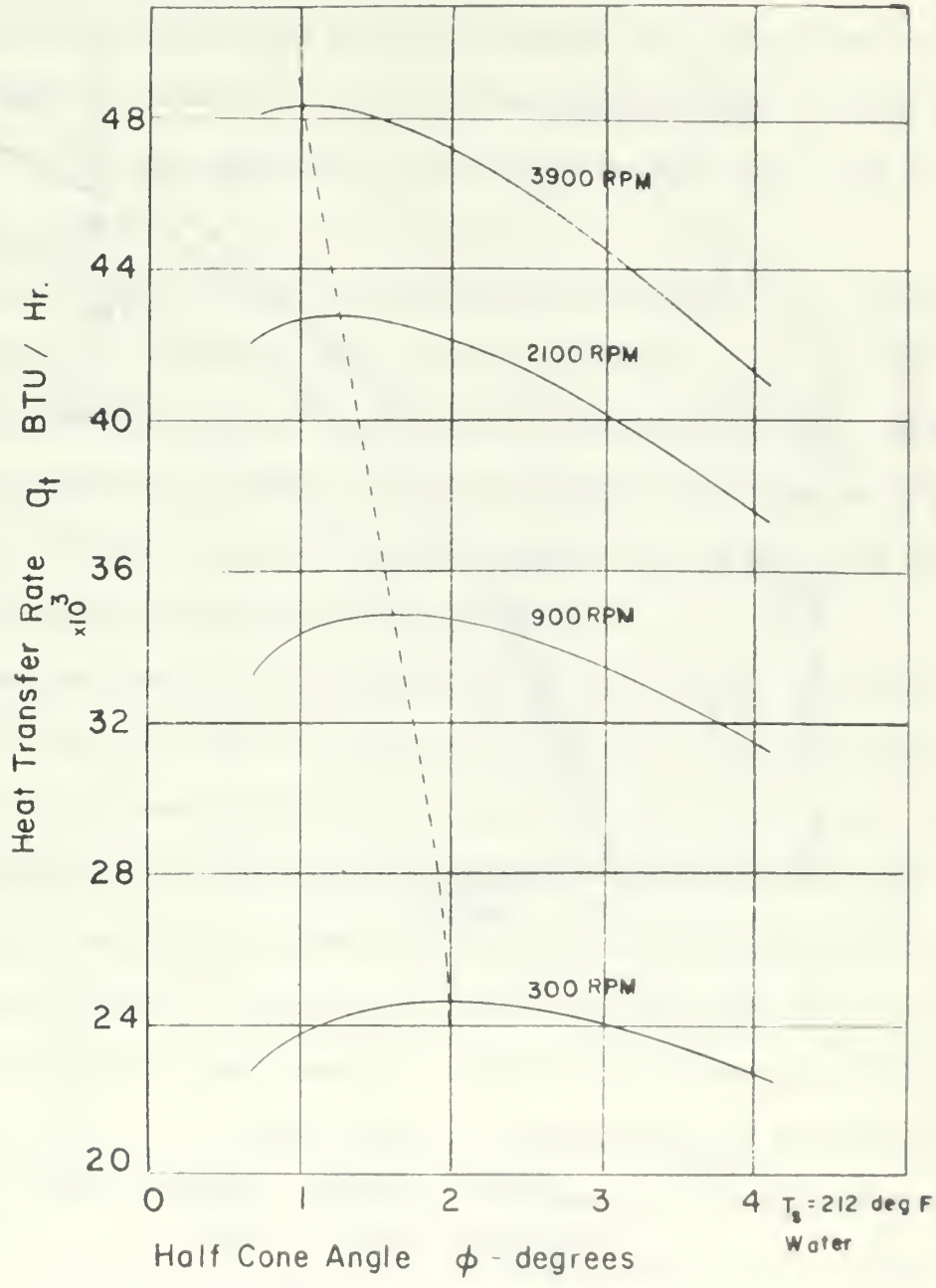

Figure 7. Condensing Limit
Heat Transfer Rate vs Half Cone Angle

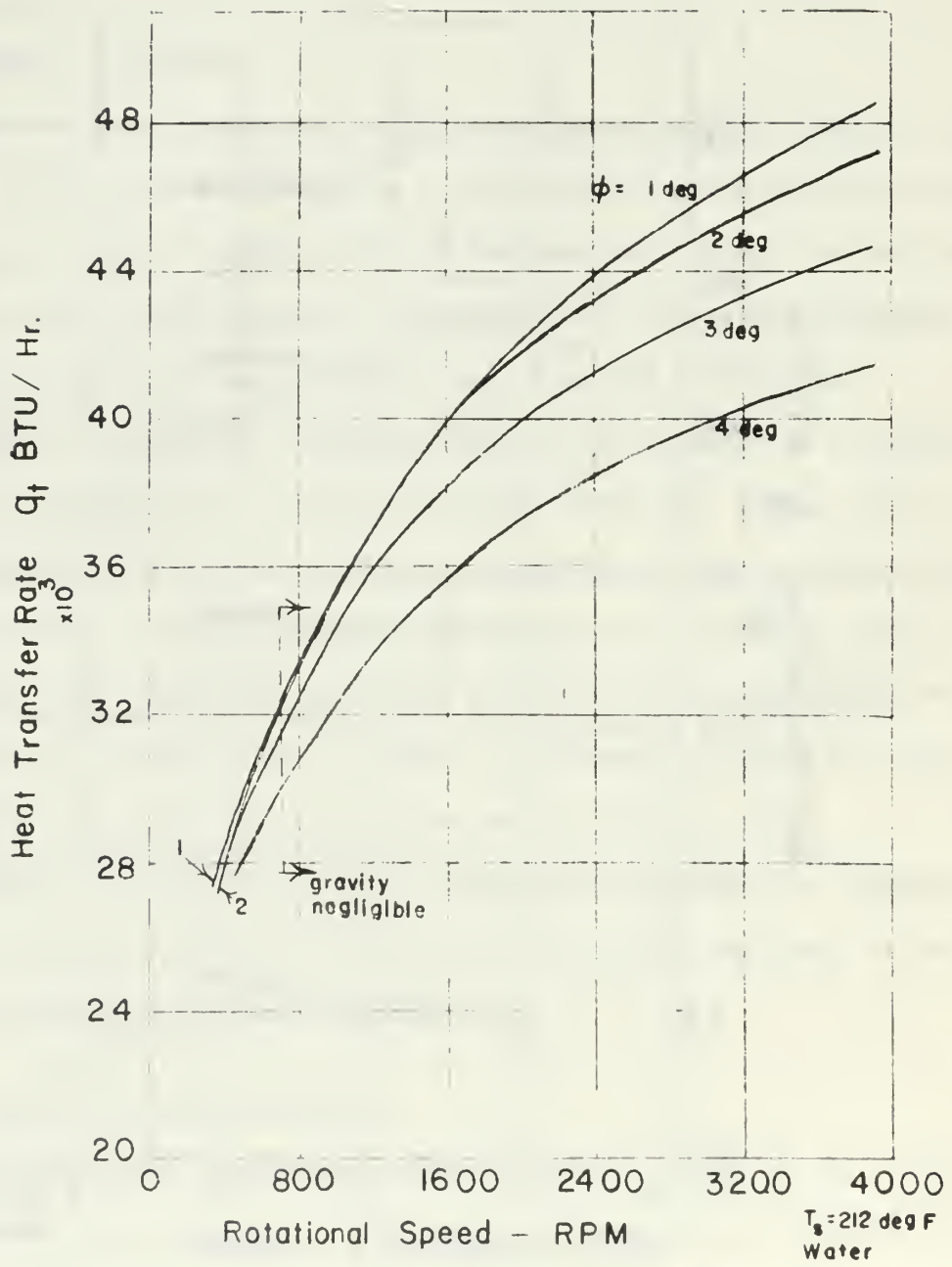

Figure 8· Heat Transfer Rate vs Rotational Speed

D. OVERALL CAPABILITY

A rotating heat pipe with the geometry shown in Fig. 5, operating at 2700 RPM, with a half cone angle of 1 degree, and using water as the working fluid was chosen to demonstrate the effects of the boiling, entrainment, sonic, and condensing limits on the maximum heat rates attainable.

The boiling limit curve was determined from equation (2), using both Kutateladze's value of K equal to .19 and Zuber's value of $\pi/24$ (.13), thus giving a range of heat rates for the boiling limit. Since the boiler surface of the rotating heat pipe may be approximated by a flat plate, for large radii of curvature, Zuber's predicted curve should be the most applicable for the model chosen.

As mentioned earlier, no suitable theory is available to predict the entrainment limit, so that the experimental results of Hewitt, Lacey, and Nicholls have been used [17]. Their data was taken from a 1.25 inch diameter stationary tube in annular flow with a counter-current air-water contact length of 9 inches. They present flooding data for the vapor mass flow rate as a function of the liquid mass flow rate. The assumption of steady state operation in the rotating heat pipe allows the Hewitt, Lacey, and Nicholls data to be entered at the condition of equal liquid and vapor mass flow rates. The mass flow rate thus obtained was then adjusted to agree with an average rotating heat pipe diameter of 2 inches and a counter-current steam-water flow condition. This adjusted mass flow rate of vapor was then used in equation (3) to give the entrainment limit.

$$q_l = \dot{m}_v h_{fg} \qquad (3)$$

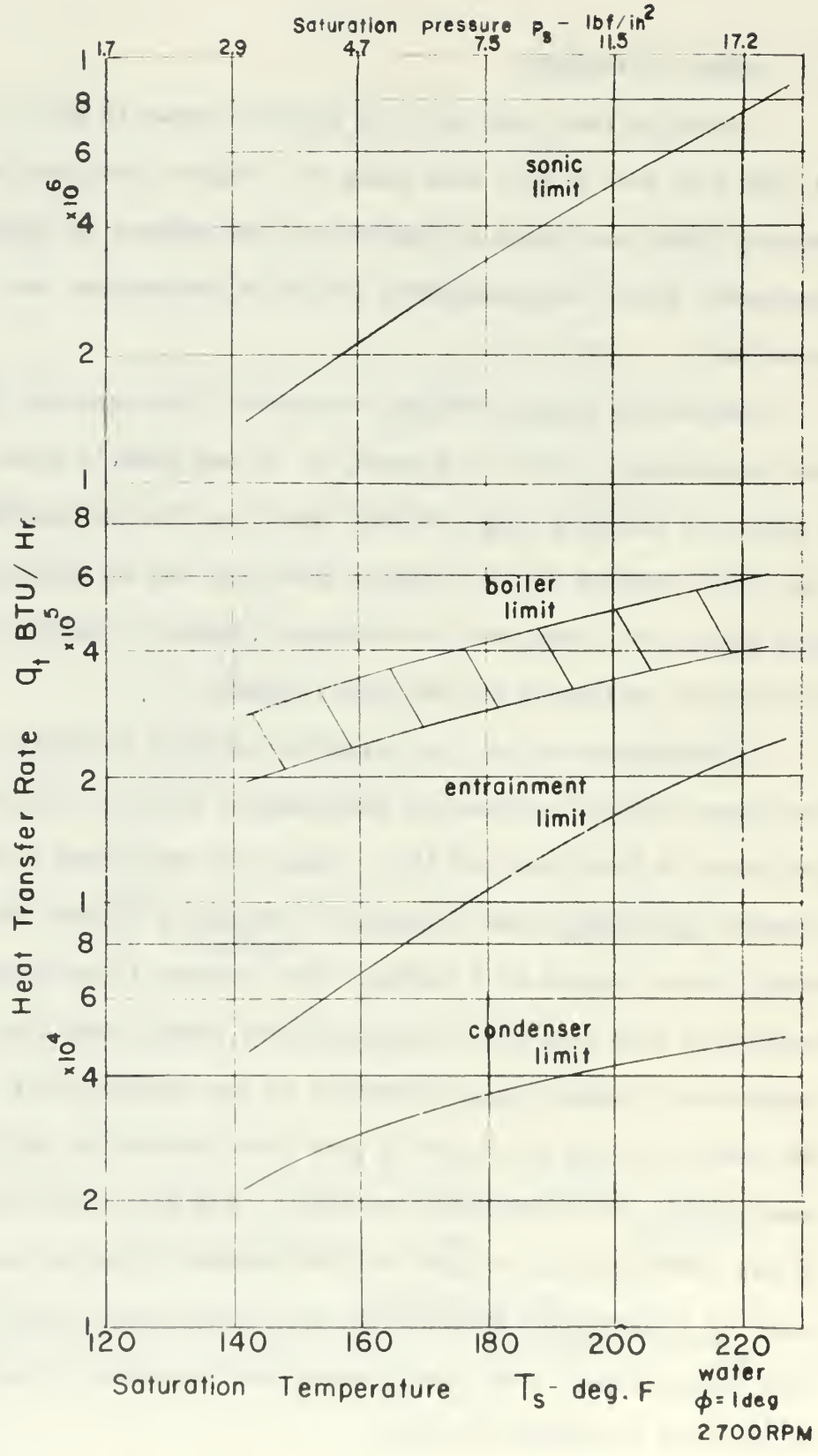

Figure 9 Heat Transfer Rate vs Saturation Temperature

Equation (5) was used in computing the sonic limit. The assumption was made that choking occurred at the exit of the boiler section for a given saturation temperature in the condenser.

The condensing limit was obtained by a solution of equations (35) and (37) as described on page 33.

Figure 9 gives the plot of the rotational heat pipes heat rate as a function of the saturation temperature for the limits just discussed.

For each of the limit curves shown in Fig. 9 there is an associated uncertainty. Even with this consideration, it is evident that the rotating heat pipe shown in Fig. 5 will be condenser limited, for a given saturation temperature. The upper limit on the heat rate attainable for a certain working fluid will generally[1] be governed by the ability of the container to withstand the saturation pressure.

---

[1] It is possible that a container could withstand a certain saturation pressure, and yet not be compatible with the associated wall temperature.

VI. CONCLUSIONS

1. The film thickness and local heat transfer coefficients for condensation on a rotating, truncated cone may be determined by a Nusselt type of analysis. The resulting film thickness and local heat transfer coefficient are not constant as for the rotating cone and disc, but vary with axial position.

2. The predicted performance for the heat pipe geometry chosen in this study, and operating with water as the working fluid, is condenser limited. For a different geometry, the entrainment limit may become the dominant limit. The sonic and boiling limits should present no practical limitation on the rotating heat pipe.

3. Of the ordinary fluids, water has the best characteristics for use as the working fluid.

4. The actual operation of the rotating heat pipe may be limited by the thermal conductance of the outside surface, (i.e., upon the method of cooling the rotating heat pipe).

VII. RECOMMENDATIONS FOR FURTHER STUDY

A. ANALYTICAL

1. An optimization study should be conducted to determine the effect of the internal geometry (boiler exit area and condenser shape as well as length) on the rotating heat pipe condensing limit.

2. The restrictions of negligible interfacial shear, negligible momentum changes in the condensate, and constant vapor pressure should be removed from the present analysis. This then would require a solution of the continuity, momentum, and energy equations for the condensate as well as the vapor. The equations of the condensate and the vapor would be coupled through the boundary condition that the shear at the interface, in each phase, must be equal.

The swirl component of the flow of condensate should also be taken into account. This would then require that the problem be solved in three-dimensions, probably through the use of spherical co-ordinates.

3. The exact location of the choked flow condition in the rotating heat pipe should be determined in order to more accurately chart the sonic limit.

4. A study should be undertaken to determine accurately the entrainment limit of the rotating heat pipe for the condenser geometry shown in Fig. 5.

B. EXPERIMENTAL

1. An experimental model should be built and the condensing heat rate limit curve for the pipe should be experimentally verified for various working fluids.

2. A comparison of filmwise and dropwise condensation in the condenser section should be made.

3. A further extension of the experimental procedure should be to have a condenser wall with axial grooves in it. This then would test the contributions of interfacial shear and swirl on the condensing limit.

APPENDIX A

SOLUTION FOR THE FILM THICKNESS, $\delta(X)$

Equation (30) may be written in the form

$$\frac{3k_f\mu_f[T_s-T_w]}{\rho_f^2\omega^2 h_{fg}\sin\phi} = 3\{R_0+X\sin\phi\}\delta^3\frac{d\delta}{dx}+2\delta^4\sin\phi \qquad \text{(A-1)}$$

Let

$$K = \frac{3k_f\mu_f[T_s-T_w]}{\rho_f^2\omega^2 h_{fg}\sin\phi}$$

$$R = R_0+X\sin\phi$$

$$U = \delta^4$$

Therefore

$$R\,dU + \left\{\frac{8}{3}U - \frac{4}{3}\frac{K}{\sin\phi}\right\}dR = 0 \qquad \text{(A-2)}$$

Now let

$$B = \frac{8}{3}U - \frac{4}{3}\frac{K}{\sin\phi}$$

This gives

$$\frac{3}{8}\frac{dB}{B} = -\frac{dR}{R} \qquad \text{(A-3)}$$

Integrating this gives

$$B^{3/8} = \frac{C}{R} \qquad \text{(A-4)}$$

where C is an arbitrary constant. Transforming equation (A-4) back into the original dimensions

$$\left\{\frac{8}{3}\delta^4 - \frac{4}{3}\frac{K}{\sin\phi}\right\}^{8/3} = \frac{C}{R_o + X\sin\phi} \tag{A-5}$$

In order to determine the arbitrary constant, C, the boundary condition $\delta = 0$ at $X = 0$ will be used. The constant, C, then is

$$C = R_o\left\{-\frac{4}{3}\frac{K}{\sin\phi}\right\}^{3/8} \tag{A-6}$$

Now substituting the original value of K and the value of C into equation (A-5), then rearranging, the final solution for δ is

$$\delta^4 = \frac{3}{2}\frac{k_f \mu_f \left[T_s - T_w\right]}{\rho_f^2 \omega^2 \sin^2\phi\, h_{fg}}\left\{1 - \left[\frac{R_o}{R_o + X\sin\phi}\right]^{8/3}\right\} \tag{A-7}$$

The solution for condensation on a rotating cone, Sparrow and Hartnett's solution, can be easily obtained by the use of the boundary condition that $\delta = 0$ at $X = 0$ for $R_o = 0$. This condition would give, from equation (A-5), that $C = 0$. The solution for delta is then the solution obtained by Sparrow and Hartnett.

APPENDIX B

SOLUTION FOR THE MEAN HEAT TRANSFER COEFFICIENT, h_m

Equation (33) may be written in the form

$$h_m = \frac{2}{L_c\left\{2R_0 + L_c \sin\phi\right\}} \left\{\frac{2}{3}\,\frac{k_f^3 \rho_f^2 \omega^2 \sin^2\phi\, h_{fg}}{\mu_f\left[T_s - T_w\right]}\right\}^{1/4} \int_0^{L_c} \left\{\frac{\left[R_0 + X\sin\phi\right]^4}{1-\left[\frac{R_0}{R_0 + X\sin\phi}\right]^{8/3}}\right\}^{1/4} dx \qquad \text{(B-1)}$$

Working with just the integral portion of equation (B-1)

$$Z = \int_0^{L_c} \left\{\frac{\left[R_0 + X\sin\phi\right]^4}{1-\left[\frac{R_0}{R_0 + X\sin\phi}\right]^{8/3}}\right\}^{1/4} dx \qquad \text{(B-2)}$$

let

$$U = R_0 + X\sin\phi$$

$$A = -R_0^{8/3}$$

Equation (B-2) then becomes

$$Z = \frac{1}{\sin\phi} \int_{R_0}^{R_0 + L_c\sin\phi} \frac{U^{5/3}}{\left[U^{8/3} + A\right]^{1/4}}\, dU \qquad \text{(B-3)}$$

let

$$V = U^{1/3}$$

Therefore

$$Z = \frac{1}{\sin\phi} \int_{R_0^{1/3}}^{V^*} \frac{3V^7}{\left[V^8 + A\right]^{1/4}}\, dV \qquad \text{(B-4)}$$

It should be noted that

$$\frac{d}{dV}\left\{V^8 + A\right\}^{3/4} = \frac{3V^7}{\left[V^8 + A\right]^{1/4}} 2\, dV$$

Carrying out the integration therefore yields

$$Z = \frac{1}{2\sin\phi}\left\{V^{8} + A\right\}^{3/4}\Bigg|_{R_0^{1/3}}^{\left\{R_0 + L_c\sin\phi\right\}^{1/3}} \qquad \text{(B-5)}$$

Finally

$$Z = \frac{1}{2\sin\phi}\left\{\left[R_0 + L_c\sin\phi\right]^{8/3} - R_0^{8/3}\right\}^{3/4} \qquad \text{(B-6)}$$

Substituting Z back into equation (B-1), the average heat transfer coefficient, h_m, is given by

$$h_m = \frac{1}{\left\{2R_0 + L_c\sin\phi\right\}}\left\{\frac{2}{3}\,\frac{k_f^3\rho_f^2\omega^2 h_{fg}}{\mu_f\left[T_s - T_w\right]\sin^2\phi\, L_c^4}\right\}^{1/4} \qquad \text{(B-7)}$$

$$\left\{\left[R_0 + L_c\sin\phi\right]^{8/3} - R_0^{8/3}\right\}^{3/4}$$

REFERENCES

1. Katzoff, S., Notes on Heat Pipes and Vapor Chambers and their Application to Thermal Control of Spacecraft, paper presented at Proceedings of Joint Atomic Energy Commission/Sandia Laboratories Heat Pipe Conference, Vol. 1, October 1966.

2. Mosteller, W. L., The Effect of Nucleate Boiling on Heat Pipe Operation, M. S. Thesis, Naval Postgraduate School, Monterey, California, April 1969.

3. Hickox, O. J., A Study of Wire Mesh Wick Characteristics in a Longitudinal Heat Pipe, M. S. Thesis, Naval Postgraduate School, Monterey, California, December 1969.

4. Gray, V. H., The Rotating Heat Pipe - A Wickless, Hollow Shaft for Transferring High Heat Fluxes, paper presented at Eleventh National Heat Transfer Conference, Minneapolis, Minnesota, August 3-6, 1969.

5. Los Alamos Scientific Laboratory of the University of California, Quarterly Status Report on the Space Electric Power R and D Program, February 26, 1969.

6. Merte, H., and Clark, J. A., "A Study of Pool Boiling in a Accelerating System," Journal of Heat Transfer, Vol. 83, Series C, No. 1, pp. 233-242, August 1961.

7. National Aeronautics and Space Administration, NASA TN D-4136, Boiling Heat Transfer Coefficient, Interface Behavior, and Vapor Quality in Rotating Boiler Operation to 475 G's, by V. H. Gray, P. J. Marto, and A. W. Joslyn, March 1968.

8. Adelberg, M., and Schwartz, S. H., Nucleate Pool Boiling at High G Levels, paper presented at the Ninth National Heat Transfer Conference A. I. Ch. E. - A.S.M.E., Seattle, Washington, August 6-9, 1967.

9. Tong, L. S., Boiling Heat Transfer and Two-Phase Flow, pp. 36-46, Wiley, 1965.

10. Kutateladze, S. C., "On the Transition to Film Boiling Under Natural Convection," Kotloturbostroenie, No. 3, pp. 10, 1948.

11. United States Atomic Energy Commission, AEC-tr-3770, Heat Transfer in Condensation and Boiling, by S. S. Kutateladze, 1952.

12. Zuber, N., Tribus, M., and Westwater, J. W., "The Hydrodynamic Crisis in Pool Boiling of Saturated and Subcooled Liquids," International Developments in Heat Transfer, A.S.M.E., New York, pp. 230-235, 1963.

13. United Kingdom Atomic Energy Authority, AEEW-R-275, The Critical Heat Flux in Pool Boiling Under Combined Effect of High Acceleration and Pressure, by W. R. Beasant and H. W. Jones, Winfrith, 1963.

14. United Kingdom Atomic Energy Authority, AEEW-R-99, Preliminary Results on the Effect of Acceleration on Critical Heat Flux in Pool Boiling, by H. J. Ivey, 1961.

15. Sun, K., and Lienhard, J. H., The Peak Pool Boiling Heat Flux on Horizontal Cylinders, College of Engineering Bulletin No. 88, University of Kentucky, Lexington, May 1969.

16. Wallis,G. B., Flooding Phenomena in Two-Phase Flow, paper presented at Two-Phase Gas-Liquid Flow, Special Summer Program, Massachusetts Institute of Technology, July 27, 1964.

17. Hewitt, G. F., Lacey, P. M. C., and Nicholls, B., Transitions in Film Flow in a Verticle Tube, paper presented at Symposium on Two Phase Flow, University of Exeter, June 21-23, 1965.

18. Joint United States-Euratom Research and Development Program, U. S. Euratom Exchange, Contract No. AT(30-1-3114-1), Two Phase Flow and Boiling Heat Transfer, by G. B. Wallis, pp. 83-84, February 1966.

19. Sparrow, E. M., and Hartnett, J. P., "Condensation on a Rotating Cone," Journal of Heat Transfer, Vol. 83, Series C, No. 1, pp. 101-102, February 1961.

20. Chapman, A. J., Heat Transfer, 2d ed., pp. 372, The Macmillan Company, 1967.

21. Cannon, J. N., and Kays, W. M., "Heat Transfer to a Fluid Flowing Inside a Pipe Rotating About its Longitudinal Axis," Journal of Heat Transfer, Vol. 91, Series C, No. 1, pp. 135-139, February 1969.

22. Sparrow, E. M., and Gregg, J. L., "A Boundary-Layer Treatment of Laminar-Film Condensation," Journal of Heat Transfer, Vol. 81, Series C, No. 1, pp. 13-18, February 1959.

23. Koh, J. C. Y., Sparrow, E. M., and Hartnett, J. P., "The Two Phase Boundary Layer in Laminar Film Condensation," Int. Journal of Heat and Mass Transfer, Vol. 2, pp. 69-82, 1961.

24. Rohsenow, W. M., "Heat Transfer and Temperature Distribution in Laminar Film Condensation," Trans. A.S.M.E., Vol. 78, pp. 1645-1648, November 1956.

25. Los Alomos Scientific Laboratory of the University of of California, Contract No. W-7405-eng. 36, Theory of Heat Pipes, by T. P. Cotter, March 1965.

26. Busse, C. A., Pressure Drop in the Vapor Phase of Long Heatpipes, paper presented at Thermionic Conversion Specialists Conference, Palo Alto, California, October 30 - November 1, 1967.

27. Nusselt, W., "Die Oberflachenkondensation des Wasserdamphes," Zeitschrift des Vereines deutscher Ingenieure, Vol. 60, pp. 541 and 569, 1916.

28. Sparrow, E. M., and Gregg, J. L., "A Theory of Rotating Condensation," Journal of Heat Transfer, Vol. 81, Series C, pp. 113-120, May 1959.

INITIAL DISTRIBUTION LIST

		No. Copies
1.	Defense Documentation Center Cameron Station Alexandria, Virginia 22314	20
2.	Library, Code 0212 Naval Postgraduate School Monterey, California 93940	2
3.	Naval Ship Systems Command, Code 2052 Via Code 31 Navy Department Washington, D. C. 20360	1
4.	Mechanical Engineering Department, Code 59 Naval Postgraduate School Monterey, California 93940	2
5.	Professor P. J. Marto Mechanical Engineering Department, Code 59Mx Naval Postgraduate School Monterey, California 93940	3
6.	LT L. J. Ballback, USN 722 Delaware Avenue Norfolk, Virginia 23513	4

DOCUMENT CONTROL DATA - R & D

(Security classification of title, body of abstract and indexing annotation must be entered when the overall report is classified)

1 ORIGINATING ACTIVITY (Corporate author) Naval Postgraduate School Monterey, California 93940	2a. REPORT SECURITY CLASSIFICATION Unclassified 2b. GROUP

3 REPORT TITLE

The Operation of a Rotating, Wickless Heat Pipe

4 DESCRIPTIVE NOTES (Type of report and, inclusive dates)

Master's Thesis; December 1969

5 AUTHOR(S) (First name, middle initial, last name)

Leonard John Ballback

6 REPORT DATE December 1969	7a. TOTAL NO. OF PAGES 54	7b. NO. OF REFS 28
8a. CONTRACT OR GRANT NO. b. PROJECT NO. c. d.	9a. ORIGINATOR'S REPORT NUMBER(S) 9b. OTHER REPORT NO(S) (Any other numbers that may be assigned this report)	

10. DISTRIBUTION STATEMENT

This document has been approved for public release and sale, its distribution is unlimited.

11. SUPPLEMENTARY NOTES	12. SPONSORING MILITARY ACTIVITY Naval Postgraduate School Monterey, California 93940

13. ABSTRACT

A Nusselt type analysis was performed during laminar film condensation on the inside of a rotating truncated cone. This analysis was employed to determine the condensing limit of a wickless heat pipe, rotating about its longitudinal axis.

Performance characteristics including the effects of geometry, rotational speed, and the characteristics of fluid are given. A comparison is made between the condensing, boiling, sonic, and entrainment limits for a given heat pipe geometry.

14 KEY WORDS	LINK A		LINK B		LINK C	
	ROLE	WT	ROLE	WT	ROLE	WT
Heat pipe, wickless						
Nusselt Theory, with rotation						
Rotating heat pipe						
Heat pipe limits						